

# Imaging ultrafast electronic motion by x-ray scattering

Gopal Dixit<sup>1,2</sup> and Robin Santra<sup>1,2,3</sup>

<sup>1</sup> Center for Free-Electron Laser Science, DESY, Notkestrasse 85, 22607 Hamburg, Germany

<sup>2</sup> The Hamburg Centre for Ultrafast Imaging, Luruper Chaussee 149, 22761 Hamburg, Germany

<sup>3</sup> Department of Physics, University of Hamburg, 20355 Hamburg, Germany

E-mail: gopal.dixit@cfel.de; robin.santra@cfel.de

**Abstract.** Time-resolved ultrafast x-ray scattering is an emerging approach to probe the temporally evolving electronic charge distribution in real-space and in real-time. In this contribution, time-resolved ultrafast x-ray scattering from an electronic wave packet is presented. It is shown that the spatial and temporal correlations are imprinted in the scattering patterns, obtained by ultrafast x-ray scattering from an electronic wave packet, which deviate drastically from the notion that the instantaneous electronic density is the key quantity being probed. Furthermore, a detailed analysis of ultrafast x-ray scattering from a sample containing a mixture of non-stationary and stationary electrons along with the role of scattering interference between a non-stationary and several stationary electrons to the total scattering signal is discussed.

## 1. Introduction

Owing to the availability of laser pulses on the sub-fs ( $1 \text{ fs} = 10^{-15} \text{ s}$ ) time scale [1, 2], much progress has been accomplished in imaging the electronic wave packet dynamics in real-time with table-top experiments in recent years [3–6]. One of the important ambitions of the emerging field of time-resolved imaging is to image the motion of an electron not only in real-time but also in real-space. Imaging the electronic motion with atomic-scale spatial and temporal resolution will help to fully understand the functionality and dynamic behavior of atoms, complex molecules and solids, for example several ubiquitous ultrafast phenomena such as bond formation and breaking, photoinduced exciton dynamics, and conformational changes and charge migration [7–9].

X-ray crystallography is a well-established method in various areas of science to obtain real-space, atomic-scale structural information of complex materials, ranging from molecular systems [10] to proteins [11]. With the tremendous advancement in technology for producing ultrashort, ultraintense and tunable x-ray pulses from free-electron lasers (XFELs), laser plasmas and high-harmonic generation [12–14], it seems feasible to obtain information about ultrafast dynamics of electrons. In recent years, using the unprecedented properties of x-rays from XFELs, several experiments have been carried out for systems ranging from atoms [15, 16], molecules [17, 18], to complex biomolecules [11, 19]. In order to image the electronic motion in real-space and in real-time, pump-probe experiment seems the most convenient approach. In such experiment, a pump pulse induces the dynamics and then subsequently a probe pulse interrogates such induced dynamics. One can perform scattering of ultrashort x-ray pulses from the temporally evolving electronic charge distribution. A series of scattering patterns obtained

by varying the pump-probe time-delay serve to image the electronic motion with atomic-scale spatial and temporal resolution. However, at this juncture a fundamental question needs to be addressed: How does an ultrashort x-ray pulse interact and scatter from a temporally evolving quantum system?

## 2. Theory

In the stationary case, the differential scattering probability (DSP), which is a key quantity in x-ray scattering, is related to the Fourier transform of the electron density  $\rho_e(\mathbf{x})$  as

$$\frac{dP}{d\Omega} = \frac{dP_e}{d\Omega} \left| \int d^3x \rho_e(\mathbf{x}) e^{i\mathbf{Q}\cdot\mathbf{x}} \right|^2. \quad (1)$$

Here,  $dP_e/d\Omega$  is the DSP for a free electron and  $\mathbf{Q}$  is the photon momentum transfer. In the recent past, the idea of obvious extension of the x-ray scattering from static to time domain was proposed by assigning an additional degree of freedom to the electron density in Eq. (1), i.e., replacing  $\rho_e(\mathbf{x})$  by  $\rho_e(\mathbf{x}, t)$  [20, 21]. Let us first employ the semiclassical theory of light-matter interaction to describe the scattering of ultrashort x-ray pulse from an electronic wave packet. In the semiclassical theory, matter is treated quantum mechanically, whereas x-ray is treated classically. According to the semiclassical theory, the DSP can be expressed as [22]

$$\frac{dP}{d\Omega} = \frac{dP_e}{d\Omega} \left| \int d^3x \rho_e(\mathbf{x}, t) e^{i\mathbf{Q}\cdot\mathbf{x}} \right|^2. \quad (2)$$

Here, we have assumed that the x-ray pulse duration is shorter than the dynamical time scale of the electronic wave packet. According to Eq. (2), the measured scattering pattern provides access to the instantaneous electron density,  $\rho_e(\mathbf{x}, t)$ , as a function of the pump-probe delay time  $t$ . Equation (2) imposes the constraint that the state of the electronic wave packet remains unchanged before and after the scattering process. But one needs an ultrashort x-ray pulse to probe electronic motion on an ultrafast time scale, which has an unavoidable bandwidth. Due to the finite bandwidth of an ultrashort x-ray pulse, it is fundamentally impossible to detect whether or not a transition between the eigenstates spanned by the wave packet, or transitions to other states closer in energy than the pulse bandwidth, has taken place. As a result, it is energetically impossible to detect inelasticity within the bandwidth. Therefore, unavoidable inelasticity leads to contributions from distinguishable final states (eigenstates) within the bandwidth, and these contributions must be summed incoherently.

In order to overcome the constraint imposed by Eq. (2), we now employ a consistent full quantum theory of light-matter interaction. In the fully quantum mechanical theory, matter and x-ray both are treated quantum mechanically and first-order time-dependent perturbation theory is employed for the interaction between matter and x-rays. The resulting expression for the DSP from a coherent, Gaussian x-ray pulse is [22]

$$\begin{aligned} \frac{dP}{d\Omega} = & \frac{dP_e}{d\Omega} \int_0^\infty d\omega_{\mathbf{k}_s} W_{\Delta E}(\omega_{\mathbf{k}_s}) \frac{\omega_{\mathbf{k}_s}}{\omega_{\mathbf{k}_{in}}} \int_{-\infty}^\infty \frac{d\tau}{2\pi} e^{-\left(\frac{2\ln 2}{\tau_l^2}\right)\tau^2} e^{-i(\omega_{\mathbf{k}_s} - \omega_{\mathbf{k}_{in}})\tau} \\ & \times \int d^3x \int d^3x' \left\langle \Psi \left( t + \frac{\tau}{2} \right) \left| \hat{n}(\mathbf{x}') e^{-i\hat{H}\tau} \hat{n}(\mathbf{x}) \right| \Psi \left( t - \frac{\tau}{2} \right) \right\rangle e^{i\mathbf{Q}\cdot(\mathbf{x}-\mathbf{x}')}. \end{aligned} \quad (3)$$

Here,  $\omega_{\mathbf{k}_{in}}$  and  $\omega_{\mathbf{k}_s}$  refer to the energy of the incident and scattered photon, respectively, and  $\tau_l$  is the pulse duration.  $\hat{H}$  represents the electronic Hamiltonian,  $\hat{n}(\mathbf{x})$  is the electron density operator and  $W_{\Delta E}(\omega_{\mathbf{k}_s})$  is a spectral window function centered at  $\omega_{\mathbf{k}_{in}}$  with a width  $\Delta E$ , which decides the range of energies of the scattered photons accepted by the detector.

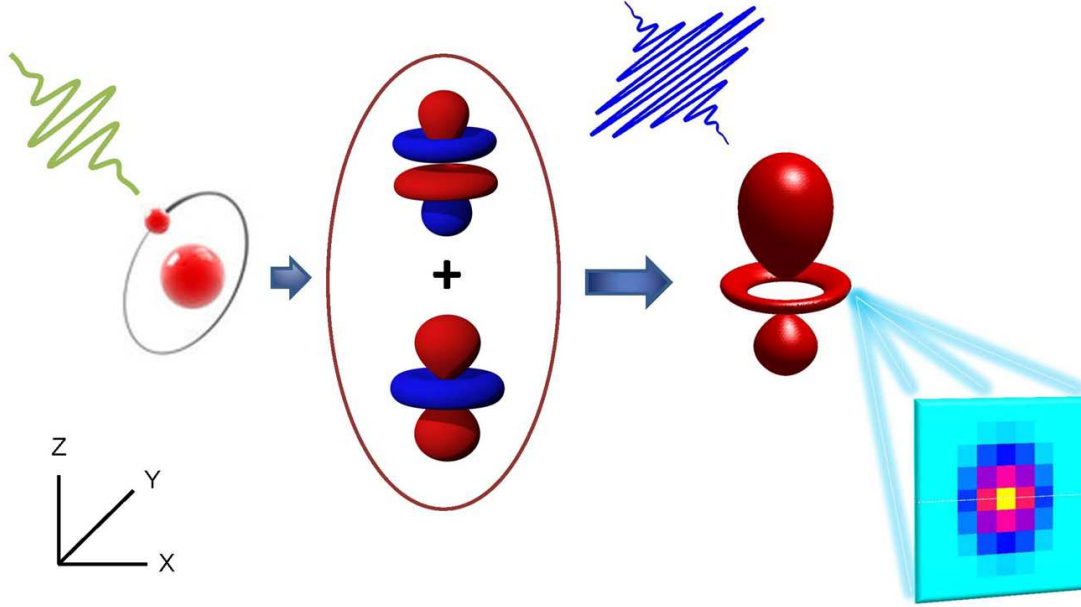


**Figure 1.** Schematic of time-resolved ultrafast x-ray scattering for imaging an electronic wave packet motion with atomic-scale spatial and temporal resolution. Adapted from Dixit *et al.* [22].

### 3. Results and Discussions

It is evident from Eqs. (2) and (3) that the semiclassical and full quantum theory provide completely different results about the electronic wave packet motion. To visually demonstrate the difference between both the equations, we calculate the scattering patterns corresponding to an electronic wave packet.

#### 3.1. Time-resolved x-ray scattering from an electronic wave packet in atomic hydrogen

A schematic scenario for imaging an electronic wave packet via ultrafast x-ray scattering is shown in Fig 1. A pump pulse with broad energy bandwidth prepares a coherent superposition with equal population of the 3d and 4f eigenstates of atomic hydrogen with projection of orbital angular momentum equal to zero. The electronic charge distribution undergoes periodic oscillation with oscillation period  $T = 6.25$  fs. The dynamically evolving charge distribution is imaged via ultrafast x-ray scattering.

As a function of the delay time at times 0,  $T/4$ ,  $T/2$ ,  $3T/4$ , and  $T$ , the scattering pattern in the  $Q_x - Q_z$  plane ( $Q_y = 0$ ) of the electronic wave packet is depicted in Fig. 2. The patterns shown in Fig. 2a and Fig. 2c are computed using Eqs. (3) and (2), respectively. The isosurface of the electronic charge distribution shown in Fig. 2b encloses  $\sim 26\%$  of the total probability and has length 14–17 Å along the  $z$ -axis and 7.5–9 Å along the  $x$  and  $y$ -axes. The wave packet is exposed to a 1-fs x-ray pulse with 4 keV photons and we assume a Gaussian photon energy detection window of width  $\Delta E = 1$  eV for the detector. Therefore, the contributions from all electronic transitions within 1 eV energy range are included incoherently for the scattering patterns shown in Fig. 2a. The patterns are calculated for  $Q_{\max} = 2 \text{ Å}^{-1}$  corresponding to a 3.14 Å spatial resolution and to a detection angle of scattered photons of up to  $60^\circ$ .

The patterns in Fig. 2a undergo spatial oscillation along  $Q_z$  and mimic the wave packet motion along  $z$  in real space as is evident from Fig. 2b. However, a careful observation reveals the

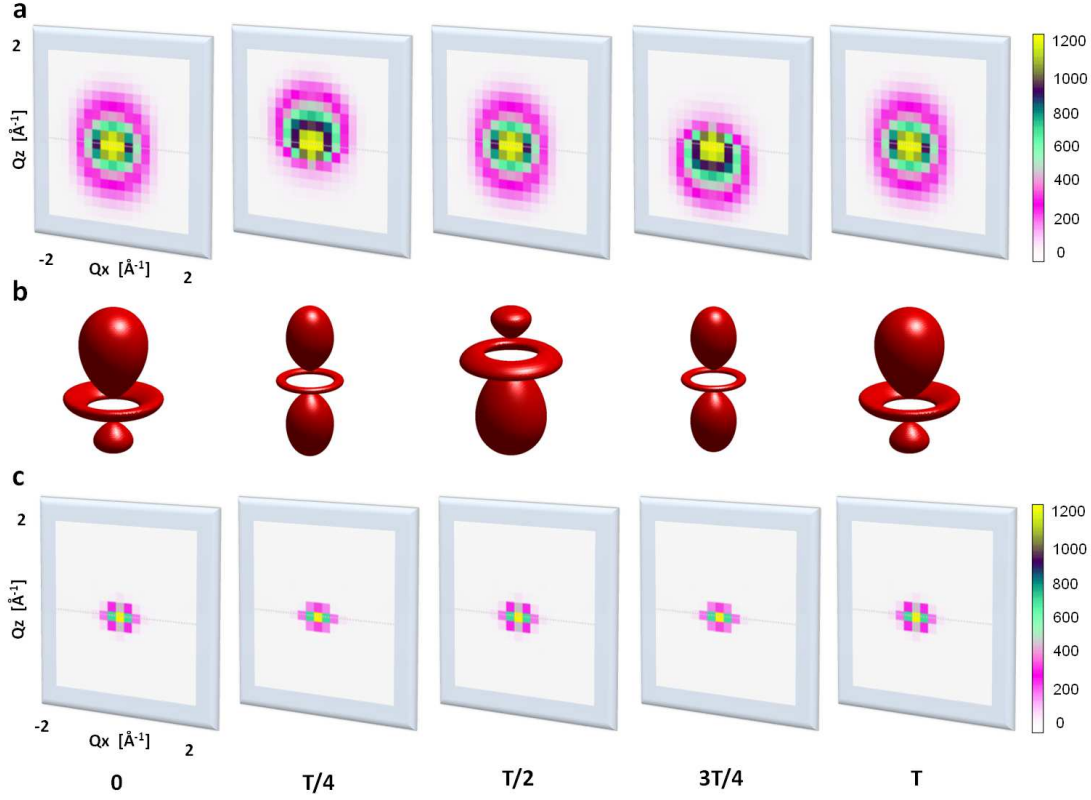


**Figure 2.** Time-resolved scattering pattern in the  $Q_x$  -  $Q_z$  plane ( $Q_y = 0$ ) and electronic charge distribution of the wave packet. (a) Scattering pattern obtained using Eq. (3), (b) isosurface of the electronic charge distribution and (c) scattering pattern obtained using Eq. (2), at the pump-probe delay times at times 0,  $T/4$ ,  $T/2$ ,  $3T/4$ , and  $T$ , where  $T = 6.25$  fs is the oscillation period. The patterns are shown in units of the Thomson scattering cross section in both cases. Adapted from Dixit *et al.* [22].

striking feature that the patterns are asymmetric when the corresponding charge distributions are symmetric and vice versa, which can be explained as follows: The electron clouds move in opposite directions at delay times  $T/4$  and  $3T/4$ , as may be seen in Fig. 2b, while the charge distributions are identical at the two times. At time  $T/4$ , the flow of the electron cloud is downwards, whereas at time  $3T/4$  the flow is upwards. This is reflected by their corresponding patterns. Moreover, the patterns in Fig. 2a are not centrosymmetric at all times, i.e., they are not equal for  $\mathbf{Q}$  and  $-\mathbf{Q}$ . This is in contrast with the centrosymmetric patterns expected from Eq. (2) as a consequence of Friedel's law [23], and shown in Fig. 2c. This counterintuitive nature of the scattering patterns arises from the fact that they are not simply related to the Fourier transform of the instantaneous electronic density, but they are related to the electronic wave packet through Eq. (3). Clearly, the patterns in Fig. 2c contain less information than the patterns shown in Fig. 2a and they miss important phase information. Therefore, the patterns calculated within the full quantum theory capture the dynamics of the *momentum distribution* of the wave packet. As a consequence, the apparent motions of the charge distributions and of the scattering patterns are phase shifted by  $90^\circ$ . On the other hand, the patterns shown in Fig. 2c do not change significantly as a function of the delay time.

Not only the scattering patterns obtained using Eqs. (2) and (3) are completely different, but

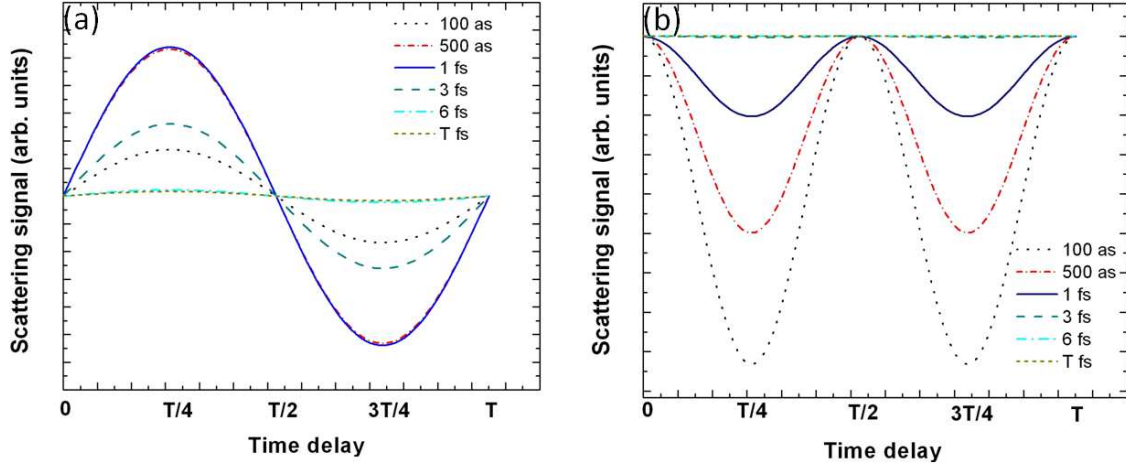


**Figure 3.** Effect of x-ray pulse duration on the scattering pattern as a function of the delay time. The scattering signal at an individual pixel of the scattering pattern obtained (a) using Eq. (3), and (b) using Eq. (2) for different pulse durations. Adapted from Dixit *et al.* [22].

the effect of the x-ray pulse duration is also different. For different pulse durations, the scattering signal at an individual pixel of the scattering pattern is shown in Fig. 3. The scattering signal calculated with Eq. (3) has the same periodicity as the corresponding wave packet dynamics. In contrast, the scattering signal calculated with Eq. (2) has the wrong periodicity. The effect of pulse duration for long pulses approaching the period of the dynamics being probed is similar for both the theories as shown in Fig. 3. In this case, the scattering signal averages out and there is no dynamical information. There is no optimum pulse duration for the signal computed with Eq. (2) in going to short pulses. The contrast as a function of time increases monotonically and for short enough pulses becomes almost constant. In contrast, the signal computed with Eq. (3) has an optimum contrast as a function of time for a pulse duration around 1-fs. For shorter pulses, the signal flattens again. The reason can be found in the matrix element in the second line of Eq. (3). This matrix element becomes independent of  $\mathbf{Q}$  for  $\tau \rightarrow 0$ , intuitively because the electron has no time to change its position. This is the only contribution summed over for a pulse of length  $\tau_l \rightarrow 0$ , and consequently, the signal becomes independent of the electronic dynamics.

### 3.2. Role of electron-electron interference

Time-resolved ultrafast x-ray scattering from a one-electron system is not a realistic situation. In reality, when a broad energy bandwidth pump pulse illuminates an  $N$ -electron system, one or few electrons form an electronic wave packet and other electrons remain stationary. In such scenario, when x-rays scatter from a mixture of stationary and non-stationary electrons, it is not possible to figure out whether the scattering occurs from the non-stationary electrons or from the stationary electrons and how the interference between non-stationary and stationary electrons contributes to the total scattering signal. Hence, it is crucial to analyze different types of contributions in the scattering process. In an  $N$ -electron system, different scattering contributions to the total scattering signal within both the theories have been rigorously analyzed by us in Ref. [24]. More specifically, the motion of a one-electron wave packet in the presence of  $N$  stationary electrons was investigated. In this case,  $N$  stationary electrons serve as reference scatterers in the total scattering signal.

It has been shown that the total signal can be factored into three main parts: first from stationary electrons, second from non-stationary electrons and third from the interference between non-stationary and stationary electrons. Also, it has been demonstrated that the scattering contributions from the stationary electrons to the signal are identical, whereas scattering contributions from the non-stationary electron are completely different in both the theories [24]. Moreover, the important contribution from the scattering interference is also different within both the theories. The scattering interference within the full quantum theory entirely depends on the energy resolution of the detector and the x-ray pulse duration. In case of extremely short pulses or negligible energy resolution, full quantum theory provides identical contributions for the scattering interference as one obtains in the semiclassical theory. In contrast to that, if the x-ray pulse is not very short in comparison to the dynamical time scale of the motion and, if the energy resolution of the detector is sufficiently high, the scattering interference within the full quantum theory does not provide identical result to the one obtained in the semiclassical theory [24].

After analyzing the role of scattering interference between non-stationary and stationary electrons, time-resolved ultrafast x-ray scattering from an electronic wave packet in helium was investigated [24]. In helium, a pump pulse excites one of the electrons from the ground state and forms a coherent superposition with equal population of the  $1s3d$  and  $1s4f$  configurations with the projection of orbital angular momentum being equal to zero. The energy difference between the  $1s3d$  and  $1s4f$  configurations is 0.66 eV, and the ground state and  $1s3d$  configurations is 23.07 eV. Also, the energy difference between non-stationary and stationary electrons is around 23 eV and they are energetically distinguishable. Therefore, any excitation from the stationary electron can be easily filtered out in the energy-resolved scattering process and hence not considered in the present case. The scattering patterns have been computed for the non-stationary electron in the presence of a stationary electron using both the theories. The time-dependent interference between the stationary and non-stationary electrons within the semiclassical theory is zero, and it is quite small in comparison to the total scattering signal in the full quantum theory. However, the time-independent interference between the stationary and non-stationary electrons contributes identically to the total signal in both the theories. The patterns are dominated by the scattering contribution from the time-independent interference within the semiclassical theory, whereas the patterns are dominated by the scattering contributions from the non-stationary electron due to Compton scattering within the full quantum theory.

### 3.3. An alternative way to image electronic motion

After analyzing the two different cases for time-resolved x-ray scattering, it has been shown that the scattering patterns encode the spatial-temporal density-density correlations, not the instantaneous electronic density. Hence, it is not easy to obtain direct information about the dynamical structural changes during the complex processes from these correlations. Whereas, if one can retrieve the instantaneous electronic density, it will provide more direct insight about these processes. Therefore, one may raise question about the possibility to image instantaneous electronic density of the wave packet in real-space and in real-time using x-ray. To answer this question, a possible way to image the instantaneous electron density via ultrafast x-ray *phase contrast imaging* has been proposed by us [25]. Ultrafast x-ray phase contrast imaging is based on the interference between two pathways – incident and scattered – of an x-ray photon. Therefore, this method does not suffer from the problem of inelastic scattering processes within the finite bandwidth of the pulse. The key quantity in this method is the Laplacian of the projected instantaneous electronic density of the wave packet. Our proposed method offers a potential to image not only instantaneous snapshots of non-stationary electron dynamics, but also the Laplacian of these snapshots which reveals the internal structures of the wave packet through local variations in the instantaneous electronic density and provides information about

the complex bonding and topology of the charge distributions in the systems [25].

#### 4. Conclusion

The illustrative example used as a proof of principle is physically simple, but lies in the time and energy range of interest corresponding to the dynamics of valence electrons in more complex molecular and biological systems. Interestingly, the scattering patterns provide an unusually visual manifestation of the quantum nature of light. This quantum nature becomes central only for non-stationary electronic states and has profound consequences for time-resolved imaging. Our present findings on time-resolved ultrafast x-ray scattering will find several important applications for exploring ultrafast dynamics in nature.

#### 5. Acknowledgments

We thank Oriol Vendrell and Jan Malte Slowik for fruitful collaboration on the topics presented here.

#### References

- [1] Hentschel M, Kienberger R, Spielmann C, Reider G A, Milosevic N, Brabec T, Corkum P, Heinzmann U, Drescher M and Krausz F 2001 *Nature* **414** 509–513
- [2] Goulielmakis E *et al.* 2008 *Science* **320** 1614
- [3] Haessler S *et al.* 2010 *Nature Physics* **6** 200
- [4] Tzallas P, Skantzakis E, Nikolopoulos L A A, Tsakiris G D and Charalambidis D 2011 *Nature Physics* **7** 781
- [5] Hockett P, Bisgaard C Z, Clarkin O J and Stolow A 2011 *Nature Physics* **7** 612
- [6] Goulielmakis E *et al.* 2010 *Nature* **466** 739
- [7] Breidbach J and Cederbaum L S 2003 *J. Chem. Phys.* **118** 3983
- [8] Kuleff A I, Breidbach J and Cederbaum L S 2005 *J. Chem. Phys.* **123** 044111
- [9] Remacle F and Levine R D 2006 *Proc. Natl. Acad. Sci. U.S.A* **103** 6793
- [10] Ihee H, Lorenc M, Kim T K, Kong Q Y, Cammarata M, Lee J H, Bratos S and Wulff M 2005 *Science* **309** 1223–1227
- [11] Chapman H N *et al.* 2011 *Nature* **470** 73
- [12] Emma P *et al.* 2010 *Nature Photonics* **4** 641
- [13] Ishikawa T *et al.* 2012 *Nature Photonics* **6** 540
- [14] Popmintchev T *et al.* 2012 *Science* **336** 1287
- [15] Young L *et al.* 2010 *Nature* **466** 56
- [16] Rohringer N *et al.* 2012 *Nature* **481** 488
- [17] Hoener M *et al.* 2010 *Phys. Rev. Lett.* **104** 253002
- [18] Berrah N *et al.* 2011 *Proc. Natl. Acad. Sci. U.S.A* **108** 16912
- [19] Seibert M M *et al.* 2011 *Nature* **470** 78
- [20] Krausz F and Ivanov M 2009 *Rev. Mod. Phys.* **81** 163
- [21] Jurek Z, Oszlanyi G and Faigel G 2004 *Euro. Phys. Lett.* **65** 491
- [22] Dixit G, Vendrell O and Santra R 2012 *Proc. Natl. Acad. Sci. U.S.A.* **109** 11636
- [23] Als-Nielsen J and McMorrow D 2011 *Elements of modern X-ray physics* (Wiley, New York)
- [24] Dixit G and Santra R 2013 *J. Chem. Phys.* **138** 134311
- [25] Dixit G, Slowik J M and Santra R 2013 *Phys. Rev. Lett.* **110** 137403